7. K. Sauer, V. K. Yachandra, R. D. Britt, M. P. Klein, in *Manganese Redox Enzymes*, V. L. Pecoraro, Ed. (VCH, New York, 1992), pp. 141–175; V. K. Yachandra *et al.*, *Science* **260**, 675 (1993); K. Wieghardt, *Angew. Chem. Int. Ed. Engl.* **28**, 1153 (1989).
8. Y. Zang, Y. Dong, L. Que Jr., K. Kauffmann, E. Münck, *J. Am. Chem. Soc.* **117**, 1169 (1995); Y. Dong *et al.*, *ibid.*, p. 2778.
9. S. Mahapatra *et al.*, *ibid.*, p. 8865.
10. K. A. Magnus *et al.*, *Proteins: Struct. Funct. Genet.* **19**, 302 (1994).
11. N. Kitajima *et al.*, *J. Am. Chem. Soc.* **114**, 1277 (1992).
12. These ideas have been discussed; for example, see (*3*); V. L. Pecoraro, M. J. Baldwin, A. Gelasco, *Chem. Rev.* **94**, 807 (1994); D. M. Proserpio, R. Hoffmann, G. C. Dismukes, *J. Am. Chem. Soc.* **114**, 4374 (1992).
13. S. Mahapatra, J. A. Halfen, E. C. Wilkinson, L. Que Jr., W. B. Tolman, *J. Am. Chem. Soc.* **116**, 9785 (1994).
14. E. I. Solomon, M. J. Baldwin, M. D. Lowery, *Chem. Rev.* **92**, 521 (1992); E. I. Solomon, F. Tuczek, D. E. Root, C. A. Brown, *ibid.* **94**, 827 (1994).
15. The Cu(I) salts with these counterions produce the peroxo complex upon low-temperature reaction with O_2 in CH_2Cl_2.
16. Single crystals of **3** · $7(CH_3)_2CO \cdot 2CH_3CN$ were grown by oxygenation and subsequent storage of a solution of $[d_{21}\text{-}L^{Bn3}Cu(CH_3CN)]SbF_6$ (containing perdeuterated benzyl groups to slow decomposition) in 1:1 CH_2Cl_2:$(CH_3)_2CO$ at −78°C. We mounted a crystal on the side of a glass capillary at low temperature using a locally designed cold stage and transferred it to the goniometer of a Siemens SMART system, with the cryogenic stream set to −150°C for data collection. The structure was refined by full-matrix least squares on F^2 for all nonhydrogen atoms; hydrogen or deuterium atoms were included and refined by use of a riding model. The asymmetric unit contains one half of the dimeric cation as well as a CH_3CN and 3.5 $(CH_3)_2CO$ solvent molecules and a rotationally disordered SbF_6^- counterion. Distance restraints were placed on the solvent molecules, the SbF_6^- counterion, and the phenyl groups of the cation to force these units to conform to their respective average substructures. Crystal data **3** · 7 $(CH_3)_2CO \cdot 2\ CH_3CN$ ($C_{70}H_{72}D_{42}Cu_2F_{12}N_8O_9Sb_2$, molecular weight M_w = 1960.70): monoclinic space group $C2/c$, a = 26.1916(6) Å, b = 15.3560(4) Å, c = 22.2705(6) Å, β (crystallographic angle between a and c) = 96.493(1)°, cell volume V = 8899.7(4) Å^3, number of formula units per cell, Z = 8. Refinement of 523 variables based on 7863 reflections and 112 restraints converged at $R1 = 0.1012$ and weighted $R2 = 0.2523$ for data with reflection intensities $I > 2\sigma(I)$ using SHELXTL 5.0.
17. D. J. Hodgson, *Prog. Inorg. Chem.* **19**, 173 (1975); S. C. Lee and R. H. Holm, *Inorg. Chem.* **32**, 4745 (1993).
18. There are two possible resonance formulations of the $[Cu_2(\mu\text{–}O)_2]^{2+}$ core: bis(μ–oxo)dicopper(III) $[Cu^{III}_2(O^{2-})_2]^{2+}$ and bis(μ-oxyl)dicopper(II) $[Cu^{II}_2(O^{1-})_2]^{2+}$. Overall, the $[Cu_2(\mu\text{–}O)_2]^{2+}$ core is oxidized by two electrons compared to the $[Cu^{II}_2(OH)_2]^{2+}$ unit, which is produced upon its decomposition (*9, 19*). Experimental assignment of the Cu oxidation state in **2** and **3** is difficult on the basis of the available data; a molecular orbital picture of the bonding in their cores derived from ab initio calculations (*9*) that avoids formal charge assignments may be most appropriate.
19. A 3:2 mixture of unperturbed L^{iPr3} and 1,4-diisopropyl-1,4,7-triazacyclononane [R. P. Houser, J. A. Halfen, V. G. Young Jr., N. J. Blackburn, W. B. Tolman, *J. Am. Chem. Soc.* **117**, 10745 (1995)] (~90% overall yield) was identified by ^1H nuclear magnetic resonance spectroscopic and gas chromatographic–mass spectrometric analysis of the solution resulting from the warming of **2** in THF followed by treatment with aqueous NH_4OH. First-order rate constants for the decomposition of **2** and **2**-d_{42} (deuterated on the isopropyl substituents) in THF were obtained at temperatures between −58° and −10°C by UV-vis spectroscopic monitoring. Analysis using the Eyring equation yielded activation parameters ($\Delta H_H\ddagger = 55 \pm 2$ kJ mol^{-1}, $\Delta S_H\ddagger = -59 \pm 8$ J K^{-1} mol^{-1}, $\Delta H_D\ddagger = 64 \pm 2$ kJ mol^{-1}, $\Delta S_D\ddagger = -50 \pm 8$ J K^{-1} mol^{-1}) and kinetic isotope effects (KIE = k_H/k_D = 34 at −50°C; 11 at 25°C). The temperature dependence of the KIE is consistent with a tunneling contribution to the reaction rate, similar to that observed for the decomposition of **3** (*9*) and a previously reported peroxo-dicobalt complex [O. M. Reinaud and K. H. Theopold, *J. Am. Chem. Soc.* **116**, 6979 (1994)].
20. Two series of experiments with $[[L^{iPr3}Cu(CH_3CN)]SbF_6] = 6.3 \times 10^{-4}$ M, $[O_2] = 5.1 \times 10^{-3}$ M or $[[L^{iPr3}Cu(CH_3CN)]SbF_6] = 1.73 \times 10^{-3}$ M, $[O_2] = 5.1 \times 10^{-3}$ M were performed between −93° and +30°C. Of these we could successfully analyze a total of 30 runs in the range −82° and −50°C by assuming a simple second-order rate constant k, first order in $[L^{iPr3}Cu(CH_3CN)]^+$ and in O_2, followed by a fast irreversible step. At higher temperatures, incomplete adduct formation, secondary decay, and significantly changing spectra precluded simple numerical treatment. In all the kinetic experiments we used a modified SFL-21 low-temperature stopped flow unit (508 diodes, 1.3-ms minimum integration time, spectral range of 300 to 720 nm) and we analyzed the results using the program KINFIT. For further details, see (*22*).
21. K. D. Karlin, N. Wei, B. Jung, S. Kaderli, A. D. Zuberbühler, *J. Am. Chem. Soc.* **113**, 5868 (1991).
22. K. D. Karlin *et al.*, *ibid.* **115**, 9506 (1993).
23. Bimetallic catalysts for the oxidation of H_2O to O_2 have been reported: J. A. Gilbert *et al.*, *ibid.* **107**, 3855 (1985); D. Geselowitz and T. J. Meyer, *Inorg. Chem.* **29**, 3894 (1990); R. Ramaraj, A. Kira, M. Kaneko, *Angew. Chem., Int. Ed. Engl.* **25**, 825 (1986); Y. Naruta, M. Sasayama, T. Sasaki, *ibid.* **33**, 1839 (1994); M. Watkinson, A. Whiting, C. A. McAuliffe, *J. Chem. Soc. Chem. Commun.* **1994**, 2141 (1994).
24. For example, see: K. D. Karlin *et al.*, *J. Am. Chem. Soc.* **110**, 1196 (1988).
25. This research was supported by the Searle Scholars Program–Chicago Community Trust (W.B.T.), the Camille and Henry Dreyfus and Sloan Foundations (fellowships to W.B.T.), the National Science Foundation (National Young Investigator Award to W.B.T.), the National Institutes of Health (grant GM33162 to L.Q., grant GM47365 to W.B.T., and a predoctororal traineeship to E.C.W.), the University of Minnesota (Doctoral Dissertation Fellowship to J.A.H.), and the Swiss National Science Foundation (A.D.Z.).

11 October 1995; accepted 15 January 1996

High-Pressure Compounds in Methane-Hydrogen Mixtures

M. S. Somayazulu,* L. W. Finger, R. J. Hemley, H. K. Mao

The effect of pressure on chemical interactions in molecular mixtures is important for problems spanning fundamental chemistry, planetary science, and materials science. Diamond-anvil cell studies reveal pressure-induced chemistry in the CH_4-H_2 system. The system, which has no known compounds at ambient conditions, formed four molecular compounds, $CH_4(H_2)_2$, $(CH_4)_2H_2$, $CH_4(H_2)_4$, and CH_4H_2, at pressures up to 10 gigapascals. These have been characterized by synchrotron single-crystal x-ray diffraction, polycrystalline x-ray diffraction, Raman spectroscopy, and visual observation. Although $CH_4(H_2)_2$ crystallizes in the $MgZn_2$-type, hexagonal Laves phase structure, $(CH_4)H_2$ has a body-centered tetragonal structure that is similar to that of Al_2Cu. The 1:1 and 1:2 compounds are stable to at least 30 gigapascals.

Chemical interactions in dense materials are important in a broad range of problems in physical science, and the nature of such interactions in mixtures of simple molecular systems has become the focus of attention recently (*1*). Fundamentally, the study of such systems under pressure is important for theories of bonding in highly condensed states, for example, the evolution of bonding states (such as van der Waals, covalent, and metallic) with compression (*2*). Technologically, investigation of such systems, particularly those containing hydrogen, is important for the design of energetic compounds and hydrogen storage materials (*3*).

A wide range of pressures (up to several hundred giga-pascals) can be created with a diamond anvil cell. High-pressure studies have been conducted to explain how simple gases and liquids mix under pressure, and some early observations showed that mixtures of helium and nitrogen formed an unusual compound with the formula $He(N_2)_{11}$ under pressures of approximately 8 GPa. Chemical compounds that are stable only at high pressure were discovered (*4*) and termed van der Waals compounds (*5–7*). In addition, high-pressure H_2-H_2O (*8*) and He-H_2O (*9*) clathrates have been discovered. Here we present a detailed study of methane-hydrogen mixtures under pressure. The study revealed four new solid compounds having H_2:CH_4 molar ratios of 1:2, 2:1, 4:1, and 1:1.

A total of 17 different compositions in the CH_4-H_2 system were studied. The initial concentration of the mixture was fixed from the partial pressures of the gases, corrected with the virial coefficients. Each mixture was loaded in the diamond anvil cell after sufficient time for homogenization had been allowed (typically a week), with a ruby chip for pressure calibration. To minimize reaction of hydrogen, Be-Cu was used as the gasket material. For all our compositions, it was found that the

---

Geophysical Laboratory and Center for High Pressure Research, Carnegie Institution of Washington, 5251 Broad Branch Road, NW, Washington, DC, 20015 USA.

*On leave from the High Pressure Physics Division, Bhabha Atomic Research Center, Bombay 400 085, India.

relative intensities of the C-H stretch and the H-H stretch (*10*) reproduced the ratio of CH_4 and H_2 within 3% in the gas and the fluid phases. It was thus possible to determine the composition of the liquid in the two-phase solid-plus-liquid region of the phase diagram, and to determine the pressure (*P*) − composition (X) relation of the liquidus. In a typical run, *P* was raised in small steps until the liquidus boundary was crossed. While within the two-phase region, the temperature (*T*) of the cell was then raised to revert back into the fluid field, and the solid was recrystallized by cooling so that a part of the sample chamber was free from the solid and consisted of only the liquid. These isochoric *P-T* scans also enabled a reproducible determination of the liquidus boundary for each composition. The laser line from an Ar^+ ion laser was focused to about 10 μm, and a spatial filter assured that the Raman signals from the two coexisting phases could be separated. The H-H peak became more intense and narrower in the solid phases; typically the line width decreased from about 20 cm^{-1} to 7 cm^{-1}. This allowed us to determine the *P* of the eutectic point (Fig. 1). Two eutectic points at 10 and 30% CH_4 were observed, as well as peritectic points at 60 and 15% CH_4.

A single solid phase was observed to form at 5.4 GPa for a starting composition of 20% CH_4. The minimum in the liquidus at this composition has been confirmed from the observed increase in freezing pressures of neighboring compositions (Fig. 1). The stoichiometry of this phase was determined to be $CH_4(H_2)_4$ (Fig. 2A shows this phase grown from a starting composition of 24% CH_4). The x-ray diffraction pattern of this phase indicated a body-centered tetragonal (bct) structure; however, we believe this pattern is due to the methane substructure. It is possible that the diffraction from the H_2 molecules could yield a primitive unit cell, but such intensities are below our detection limit. Incongruent melting of this phase was observed at 6.1 GPa and 298 K, at which pressure the solid changes stoichimetry through the reaction $CH_4(H_2)_4$ (S) → $CH_4(H_2)_2$ (S) + *L* (S, solid; *L*, liquid). At high temperatures, this transition was also accompanied by a change in *dP*/*dT* in the isochoric *P-T* scans. X-ray intensity data for this phase were collected at 6.2 GPa and indicated a hexagonal unit cell with a = 5.414 (2), c = 8.855 (8) Å, and volume V = 224.8 (3) Å^3, for a coordination number Z = 4. The space group was identified to be $P6_3/mmc$. If the equation of state of H_2 (*5*) and CH_4 (*6*) is used, the volume is occupied by about 4 CH_4 and 8 H_2, with a 1% excess volume of mixing. The structure is that of a $MgZn_2$ (Laves phase) structure (*7*). Figure 3A shows where the H_2 molecules occupy the Zn sites and the CH_4 molecules occupy the Mg sites. Above 6.7 GPa, another solid with the composition CH_4H_2 was formed (Fig. 2B). It has a hexagonal crystal structure similar to that of $CH_4(H_2)_2$, with a smaller *c*/*a*

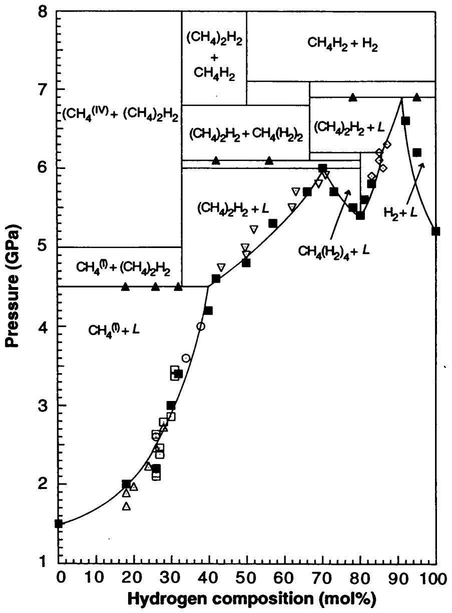

Fig. 1. The *P-X* phase diagram of the binary molecular system H_2–CH_4 at 298 K. The solid symbols denote the freezing pressures (liquidus boundary) and the pressures at which complete solidification (eutectic pressures) is observed. The open symbols represent the composition determined from the liquid in the two-phase solid-plus-liquid regions.

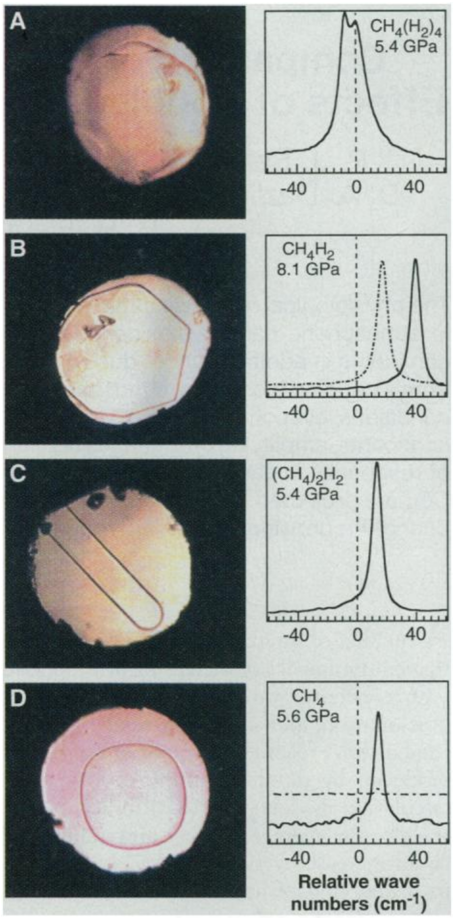

Fig. 2. Photomicrographs of phases in the sample chamber, about 150 μm in diameter, with corresponding Raman spectra of the H-H stretching mode shown for each phase. The spectra are plotted relative to the frequency of the $Q_1(J)$ vibron of pure hydrogen at that pressure (vertical dashed line). (**A**) $CH_4(H_2)_4$ at 5.4 GPa. The doublet indicates that the spectrum was collected from a two-phase mixture: solid $CH_4(H_2)_4$ and hydrogen-rich liquid. (**B**) CH_4H_2 at 8.1 GPa in a solid H_2 medium. The Raman spectra were collected from a 50-50 starting composition. The mode from $(CH_4)_2H_2$ is shown by a dashed line, and the mode from CH_4H_2 is shown by a solid line. (**C**) $(CH_4)_2H_2$ at 5.4 GPa. The hydrogen $Q_1(J)$ mode occurs at a higher frequency in this compound as compared with that in pure hydrogen at this pressure. (**D**) Pure methane at 5.6 GPa in the solid medium $(CH_4)_2H_2$. The horizontal dashed line is the spectrum collected from the pure methane region.

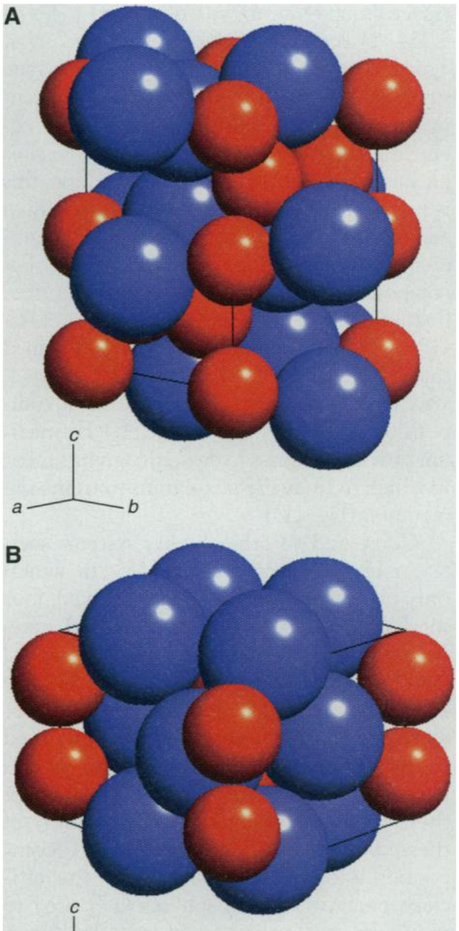

Fig. 3. (**A**) Crystal structure of the compound $CH_4(H_2)_2$. The H_2 and CH_4 molecules are represented as spheres because they appear to be orientationally disordered at these pressures. This phase is stable between 5.8 and 7 GPa, above which it continues to be hexagonal but changes stoichiometry. (**B**) Crystal structure of the compound $(CH_4)_2H_2$. Raman measurements on this solid indicate that it is stable up to at least 30 GPa.

ratio but major changes in the relative intensities of the (100), (200), and (300) reflections, which suggests a different space group (*11*). The observed unit cell parameters at 7.9 GPa are a = 5.305 (2), c = 8.633 (6) Å, and V = 210.4 (3) Å^3. A stoichiometry of 1:1 CH_4:H_2 yields a much larger volume of mixing (12%). The observed cell parameters and c/a ratio are consistent with the wurzite structure (B4) for this compound. The spectroscopic signature of this transition is the positive shift of the $Q_1(J)$ hydrogen vibron with respect to the one in the pure solid at this pressure (Fig. 2B). Raman measurements of the H_2 vibron from this phase up to 30 GPa showed no changes, indicating that the compound is stable to at least 30 GPa (*12*).

The methane-rich compound $(CH_4)_2H_2$ crystallizes as a needle-shaped crystal (Fig. 2C). X-ray data were collected on a single crystal grown from a starting composition of 40% H_2 at 5.6 GPa. The unit cell was bct (space group $I4/mcm$) with a = 7.231 (1), c = 5.934 (1) Å and V = 310.3 (1) Å^3, for $Z = 4$. This structure is similar to the Al_2Cu-type structure (*13*), with the CH_4 molecules occupying the Al sites and the H_2 molecules occupying the Cu sites (Fig. 3B). Based on simple considerations of hard sphere packing, this is not surprising because the Al_2Cu family of alloys has a similar atomic (molecular) diameter ratio in the range 1.13:1 to 1.61:1. For compositions above 35% H_2, methane froze first; and above the peritectic pressure of 4.5 GPa, the compound $(CH_4)_2H_2$ formed through the peritectic reaction $CH_4\ (S) + L \rightarrow CH_4\ (S) + (CH_4)_2H_2\ (S)$. With a composition of 20% H_2, the soft $(CH_4)_2H_2$ medium provided a quasi-hydrostatic environment in which to study the phase transitions in pure methane (Fig. 2D).

Compared to other binary systems such as Ar-H_2 (*14*) and He-Ne (*15*), in which only one compound has been observed, four solid phases have been documented here. Two of the stoichiometric solids observed fall close to the compounds observed in the N_2-CH_4 system (*16*). However, in contrast to that system, no unmixing was observed in the fluid phase. This comparison reveals a number of systematics in the structures of these new compounds. The formation of these van der Waals (molecular) compounds is essentially dictated by the efficient packing of hard spheres (*17*) used to rationalize the structures of metallic alloys. For $CH_4(H_2)_2$, the structure is similar to that of $Ar(H_2)_2$ (*14*), as is expected because the diameter ratios are fairly close to 1.22:1, which satisfies the condition for the formation of a $MgZn_2$ (Laves phase) structure (*7*).

REFERENCES AND NOTES

1. P. Loubeyre, in *Molecular Systems under High Pressure*, R. Pucci and G. Piccitto, Eds. (Elsevier, Amsterdam, Netherlands, 1991), pp. 245–262; J. A. Schouten, *J. Phys. Condens. Matter* **7**, 469 (1995).
2. H. K. Mao and R. J. Hemley, *Rev. Mod. Phys.* **66**, 671 (1994).
3. J. H. van der Waals, *Ann. N.Y. Acad. Sci.* **715**, 29 (1994).
4. W. L. Vos *et al.*, *Nature* **358**, 46 (1992).
5. R. J. Hemley *et al.*, *Phys. Rev. B* **42**, 6458 (1990).
6. R. M. Hazen, H. K. Mao, L. W. Finger, P. M. Bell, *Appl. Phys. Lett.* **37**, 288 (1980).
7. W. Hume-Rothery, S. E. Smallman, C. W. Haworth, *The Structure of Metals and Alloys* (Institute of Metals and Alloys, London, 1969).
8. W. L. Vos, L. W. Finger, R. J. Hemley, H. K. Mao, *Phys. Rev. Lett.* **71**, 3150 (1993).
9. D. Londono, W. F. Kuhs, J. L. Finney, *Nature* **332**, 141 (1988).
10. Normalized with respect to the gas phase scattering strengths of the C–H $\nu_3(A_1)$ mode at 2914 cm^{-1} and the H–H Q_1(J) mode at 4156 cm^{-1}.
11. M. S. Somayazulu, R. J. Hemley, L. W. Finger, H. K. Mao, in preparation.
12. M. S. Somayazulu, A. F. Goncharov, R. J. Hemley, H. K. Mao, L. W. Finger, *Bull. Am. Phys. Soc.*, in press.
13. E. E. Havinga, H. Damsma, P. Hokkeling, *J. Less Common Met.* **27**, 169 (1972).
14. P. Loubeyre, R. LeToullec, J.-P. Pinceaux, *Phys. Rev. Lett.* **72**, 1360 (1994).
15. P. Loubeyre, M. Jean-Louis, R. LeToullec, L. Charon-Gerard, *ibid.* **70**, 178 (1993).
16. J. A. Schouten, M. G. E. von Hinsberg, M. I. M. Scheerboom, J. P. J. Michels, *J. Phys. Condens. Matter* **6**, A187 (1994).
17. M. D. Elkridge, P. A. Madden, D. Frenkel, *Nature* **365**, 35 (1993).

12 October 1995; accepted 16 January 1996

Comparison of Radiative and Physiological Effects of Doubled Atmospheric CO_2 on Climate

P. J. Sellers, L. Bounoua, G. J. Collatz, D. A. Randall,
D. A. Dazlich, S. O. Los, J. A. Berry, I. Fung, C. J. Tucker,
C. B. Field, T. G. Jensen

The physiological response of terrestrial vegetation when directly exposed to an increase in atmospheric carbon dioxide (CO_2) concentration could result in warming over the continents in addition to that due to the conventional CO_2 "greenhouse effect." Results from a coupled biosphere-atmosphere model (SiB2-GCM) indicate that, for doubled CO_2 conditions, evapotranspiration will drop and air temperature will increase over the tropical continents, amplifying the changes resulting from atmospheric radiative effects. The range of responses in surface air temperature and terrestrial carbon uptake due to increased CO_2 are projected to be inversely related in the tropics year-round and inversely related during the growing season elsewhere.

A number of simulation studies have investigated the impact of increasing atmospheric CO_2 concentration on the energy balance, precipitation, and surface air temperature of the Earth. A recent assessment of the results produced by different atmospheric general circulation models (AGCMs) indicates that the globally averaged surface air temperature could increase by 1.5° to 4.5°C in response to a doubling of atmospheric CO_2 (*1*). In almost all cases, the impacts of increasing CO_2 are conventionally associated with changes in the radiation and energy balances; physiologically induced effects on climate are ignored. In this report we investigate the potential for additional warming over the continents as a result of the physiological response of terrestrial vegetation when exposed to an equilibrium doubling in atmospheric CO_2 concentration.

Terrestrial vegetation takes up CO_2 for photosynthesis through small pores in the leaf surfaces called stomates. At the same time, water vapor from the leaf interior diffuses out through the stomates to the atmosphere (transpiration). Plants continuously adjust the widths of their stomatal apertures, apparently to enhance CO_2 uptake for a given evaporative loss of leaf water (*2*). Leaf stomatal conductance to water vapor transfer appears to be sensitive to variations in net photosynthetic rate, and hence to light intensity, temperature, soil moisture, and atmospheric CO_2 concentration, as well as to changes in humidity and CO_2 concentration at the leaf surface. Leaf-scale models of net photosynthetic assimilation, A, and stomatal conductance, g_s, have been formulated to describe these relations [see, for example, (*3*)].

The physiological effects on climate caused by increasing atmospheric CO_2 result from the dependence of photosynthesis and stomatal conductance on CO_2 partial pressure (Fig. 1). Short-term exposure of C_3 plants to 2 × CO_2 (a doubling of the CO_2

P. J. Sellers, G. J. Collatz, S. O. Los, C. J. Tucker, National Aeronautics and Space Administration, Goddard Space Flight Center (NASA GSFC), Biospheric Sciences, Code 923, Greenbelt, MD 20771, USA.
L. Bounoua, Universities Space Research Association, NASA GSFC, Biospheric Sciences, Code 923, Greenbelt, MD 20771, USA.
D. A. Randall, D. A. Dazlich, T. G. Jensen, Department of Atmospheric Sciences, Colorado State University, Fort Collins, CO 80523, USA.
J. A. Berry and C. B. Field, Department of Plant Biology, Carnegie Institution of Washington, Stanford, CA 94305, USA.
I. Fung, Department of Earth and Ocean Sciences, University of Victoria, Victoria, British Columbia, V8N 3X3, Canada.